International Journal of Pharmaceutics 427 (2012) 242–251

Contents lists available at SciVerse ScienceDirect

International Journal of Pharmaceutics

journal homepage: www.elsevier.com/locate/ijpharm

PCL films incorporated with paclitaxel/5-fluorouracil: Effects of formulation and spacial architecture on drug release

Hao-Jun Rong, Wei-Luan Chen, Sheng-Rong Guo*, Lei Lei, Yuan-Yuan Shen

School of Pharmacy, Shanghai Jiao Tong University, Shanghai 200240, China

ARTICLE INFO

Article history:
Received 20 October 2011
Received in revised form 12 January 2012
Accepted 5 February 2012
Available online 14 February 2012

Keywords:
Film
5-Fluorouracil
Paclitaxel
PCL
Drug release

ABSTRACT

The bi/tri-layered poly(ε-caprolactone) (PCL)-based films co-loaded with 5-fluorouracil (5-FU) and paclitaxel (PTX) are presented for biodegradable film-based stent application. A gradient elution HPLC analytical method was used for simultaneous quantification of 5-FU and PTX. Scanning electron microscopy (SEM) was performed to observe the microscopic architecture and morphologies, and X-ray diffraction (XRD) was employed for analyzing the physical state of the components in the single layer film. Horizontal cells diffusion test results indicated that the multi-layered structure endowed the film with drug release in unidirectional pattern. The *in vitro* release results showed that drug release was dependent on the drug loading, the ratio of 5-FU/PTX, the composition of surface layer, as well as the addition of hydrophilic PEG. The cytotoxicity results indicated that the PCL-based films co-loaded with 5-FU and PTX could effectively inhibit the proliferation of Eca-109 cells. The *in vivo* drug release results showed that the *in vivo* drug release was highly correlative with the *in vitro* drug releases. This study provided PCL-based films co-loaded with 5-FU and PTX with great potential for anti-tumor stent application, due to their unidirectional and rate-tunable drug release characteristics and dual drug loading capacity.

1. Introduction

5-Fluorouracil (5-FU) and paclitaxel (PTX) are both widely used in the treatment of cancer (Gupte and Ciftci, 2004). 5-FU inhibits the proliferation of tumor cells by interfering with nucleic acid metabolism and inhibiting DNA synthesis of tumor cell (Longley et al., 2003). PTX inhibits division and proliferation of tumor cell by promoting microtubule assembly and stabilizing tubulin polymer formation (Sugimura et al., 2004). Thus, 5-FU and PTX act their effects at different phases of cell cycle. Since there is no cross-resistance between 5-FU and PTX (Gupta, 1985), combinational use of the two drugs in clinical has been widely reported (Feng et al., 2004; Lee et al., 2006; Watari et al., 2008). Currently, long-term systemic injection of 5-FU and PTX, which are commonly used in clinical practice, will bring about adverse reaction (Monsuez et al., 2010). Accordingly, local drug delivery devices are a more preferable option for delivering PTX or 5-FU. Many studies on local drug delivery for single PTX or 5-FU have been reported (Lei et al., 2011b; Liu et al., 2011).

Recently, more attention has been paid to drug-eluting stent (DES) due to its dual functions of supporting the lumen and treating local intraluminal tumor or preventing the restenosis by releasing drug (Guo et al., 2009). Based on the materials used for making of DESs, stents can be divided into non-biodegradable and biodegradable ones. Non-biodegradable DESs have to be removed by a second surgery when the treatment period ends, and they are partly responsible for late adverse effects and pathologic reactions (Ako et al., 2007), which may impose extra pains on patients and worsen the patients' quality of life. Therefore, biodegradable DESs could be more helpful and preferable (Tsuji et al., 2003). Many biodegradable DESs based on biocompatible polymers have been investigated and clinically tested (Zilberman and Eberhart, 2006), and the results are positive (Waksman and Wakabayashi, 2010).

Poly(ε-caprolactone) (PCL), a biodegradable aliphatic polyester, has many advantageous properties, including good drug permeability, good biocompatibility, good anti-fatigue capability, good elastic performance, and low cost relative to other biodegradable polyesters (Little et al., 2009). Also, PCL is one of the polymers that have been approved by Food and Drug Administration (FDA) to be used *in vivo* (Rohner et al., 2002). Being compatible with many drugs and with a low melting temperature (60 °C) (Sinha et al., 2004), PCL ensure the possibility of making DESs that not only provide support but can also deliver therapeutic agents.

So far, some biodegradable DESs based on PCL have been investigated (Lei et al., 2011a), but few studies have reported the co-loading with 5-FU and PTX in PCL-based stents. In this study, a series of multi-layered PCL films co-loaded with 5-FU and PTX were designed and prepared. We explored a variety of properties

* Corresponding author. Tel.: +86 21 3420 4792; fax: +86 21 3420 4793.
E-mail address: srguo@sjtu.edu.cn (S.-R. Guo).

0378-5173/$ – see front matter © 2012 Elsevier B.V. All rights reserved.
doi:10.1016/j.ijpharm.2012.02.007

of the films, including drug permeability, drug release behaviors, evolution of microstructures and crystalline states, to examine the feasibility of this film-based polymeric biodegradable stent.

2. Materials and methods

2.1. Materials

5-FU was purchased from Nantong Jinghua Pharmaceutical Co., Ltd. (Nantong City, China) and PTX was obtained from Xi'an Haoxuan Biological Technology Co., Ltd. (Xi'an, China). PCL 80K (Mw = 80,000) was purchased from Shenzhen BrightChina Industrial Co., Ltd. (Shenzhen, China). Polyethylene glycol (PEG, Mw = 6000) was obtained from SinopharmChemical Reagent Co., Ltd. (Shanghai, China). HPLC grade methanol was purchased from Shanghai Xingke Biochemistry Co., Ltd. Deionized water was purified by a Milli-Q water purifier system from Millipore (Bedford, MA, USA). All other chemicals were of analytical grade and used as received.

2.2. Film preparation

The single layered films used for consisting the bi/tri-layered film were prepared as follows: first, various combinations of ingredients were fed into the chamber of a HAAKE MiniLab II twin screw extruder (Thermo Fischer Scientific, Waltham, MA) and blended thoroughly at 90 °C and a rotor speed of 30 rpm for 30 min; then, the resulting blends were hot-pressed into films with defined thickness on a compression molding machine (XLB-D, Shanghai No. 1 Rubber Machine Factory) at 100 °C, followed by cooling to room temperature. The compositions of single layered films are listed in Table 1. To prepare bi/tri-layered film, the two/three single layers were agglutinated together layer by layer with toluene as the agglutinant and then pressed under the pressure of 0.25 kg/cm^2 for 5 min to form a robust bi-layered/tri-layered structure. The resulting bi/tri-layered films were left in a vacuum oven at 35 °C for 3 d to remove the residual toluene.

2.3. HPLC

5-FU and PTX concentrations were simultaneously determined by our previously reported HPLC method (Chen et al., 2012). The waters system consisted of a photodiode array detector (2998), a binary HPLC pump (1525) and an autosampler (2707). A Venusil C18 reversed phase column (particle size 5 μm, 4.6 mm × 250 mm) was used. The UV detection were performed at 266 nm (for 5-FU) and 227 nm (for PTX) with the column temperature maintained at 30 °C, and the analytical signal was monitored and integrated by Empower™ 2 chromatography software. The mobile phase was composed of solvent A (100% methanol) and solvent B (0.5% H_3PO_4 aqueous solution). The flow rate was 1 mL/min and the injection volume was 50 μL. Linear gradient elution was employed with a 18.5 min run time; the gradient was: 0–3 min, maintain at 6% A after injection; 3–3.5 min, linear gradient from 6 to 75% A; 3.5–16 min, maintain at 75% A; 16–16.5 min, linear gradient from 75 to 6% A; 16.5–18.5 min, maintain at 6% A (Chen et al., 2012). All sample solution was filtered through a 0.45 μm filter membrane before injection.

Table 1
Compositions of the single layered films.

Film	Composition (w/w, %)			
	5-Fu	PTX	PEG	PCL
I	50	–	–	50
II	–	50	–	50
III	10	40	–	50
IV	40	10	–	50
V	–	20	–	80
VI	–	20	20	60
VII	–	50	10	40
VIII	–	–	–	100
IX	–	–	15	85

2.4. In vitro release

For *in vitro* release, the bi/tri-layered film was cut into 1 cm × 1 cm squares. Each square was placed in a tube containing 15 mL of phosphate buffered saline (pH 7.4) (PBS) with 1% sodium dodecyl sulfate (SDS) (w/v) to keep sink condition. The tubes were placed in a shaking water bath at 37 °C with a shaking speed of 100 rpm. At defined time points, the release medium was completely withdrawn and replaced by an equal volume of fresh PBS. The PTX and 5-FU concentrations in the release medium were assessed by HPLC. Prior to HPLC determination, the collected drug release medium was diluted with a certain volume of ethanol.

2.5. Horizontal cells diffusion

Permeations of PTX and 5-FU from the drug-loaded layer and PCL backing layer were explored by using horizontal V-C cells (Shanghai Kaikai Scientific Technology, Shanghai, China). The bi-layered film was mounted between donor and receiver chambers of a set of horizontal cells which provided an effective diffusion area of 0.78 cm^2. Both the donor and receiver chambers were filled with 4 mL PBS (pH 7.4) with 1% SDS (w/v). The temperature of PBS was kept at 37 °C and constantly stirred with magnetic stir bars at a rate of 250 rpm to minimize the boundary effect. At defined time points, the medium in the donor and receiver chambers was completely withdrawn for HPLC examination and replaced with 4 mL fresh PBS.

2.6. X-ray diffraction (XRD)

XRD analyses of the single layered films, PTX particles, 5-FU powders and PEG were obtained using an X-ray diffractometer (D/max 2200, Rigaku, Japan) equipped with Cu Kα radiation source (40 kV, 20 mA). The XRD traces were scanned at a rate of 5°/min over a 2θ range of 5–45°.

2.7. Scanning electron microscopy (SEM)

The cross-section and surface morphologies of the films were imaged by a JSM-7401F scanning electron microscope (SEM) (JEOL, Tokyo, Japan). The cross-section of film was obtained by freeze fracturing the film in liquid nitrogen. Prior to imaging, the samples were placed on a metal sample holder and sputter coated (Emitech K-575 Sputter Coater) with gold–palladium at a thickness of 7.5 nm. SEM images were obtained at 1 kV accelerating voltage and 20 mA current.

2.8. 3-(4,5-Dimethylthiazol-2-yl)-2,5-diphenyltetrazolium bromide (MTT) assay

Drug free PCL film (serving as control) and Films 1–4 were cut into 0.8 cm × 0.8 cm squares and submerged in PBS under the same condition as those described in Section 2.4. The films were taken out from the release media after 0 h, 10 h, 24 h, 72 h, and 120 h after drug release, respectively, dried and sterilized by UV for cytotoxicity assay.

Eca-109 cells (obtained from the Cell Bank of Type Culture Collection of Chinese Academy of Sciences, Shanghai, China) were

seeded in 48-well plates (1×10^5 cells/well), with each well containing 200 μL of RPMI-1640 medium supplemented with 10% fetal bovine serum (FBS), 100 units/mL penicillin and 100 μg/mL streptomycin. After incubating for 12 h, the medium was replaced with 1.2 mL of fresh one. Subsequently, the sterilized films were carefully placed in these wells in a way that the films were completely submerged in the culture medium but not resting on the cells. After co-incubation with cells for 48 h, the culture medium and films were removed and the cells were washed with PBS (pH 7.4). Then, 400 μL of MTT dissolved in FBS-free RPMI-1640 medium (0.5 mg/mL) was added to each well, and cultivated for 4 h at 37 °C and 5% CO_2. Then, the supernatant were removed carefully, and 400 μL of dimethyl sulfoxide (DMSO) was added to each well to dissolve the formed formazan thoroughly.

Absorbance values were measured with a SpectraMax® M5/M5^e microplate reader (Molecular Devices, USA) at 570 nm and corrected by subtracting the values measured at 650 nm. Cell viability was expressed as the ratio of the amount of formazan determined for cells treated with Films 1–4 to that for control cells, and the cell inhibition rates were calculated according to the following formula:

$$\text{Cell inhibition rates} = \left(1 - \frac{A_{570-650}\ \text{mean of the test hole}}{A_{570-650}\ \text{mean of the control}}\right) \times 100\%$$

2.9. In vivo release in mice

Films 3 and 4 were cut into discs with a diameter of 1.2 cm for implantation and each disc was weighed accurately. Prior to implantation, the discs were sterilized under UV light for 3 h. Thirty five-week-old female Kunming mice (obtained from Shanghai SLAC Laboratory Animal Co., Ltd., Shanghai, China) were randomized into Group A and Group B and implanted with the discs of Films 3 and 4, respectively.

The implantation procedure was as follows: firstly, all mice were anesthetized by intraperitoneal injection of ethyl aminoformate aqueous solution (20%, w/v), then a small incision was made at the left planes of the dorsal area of the mice (Cheng et al., 2010a). Subsequently, discs were implanted into the subcutaneous tissue and the incision was sutured. After the implantation, all animals were placed in a heated recovery chamber until conscious.

At determined time points after the implantation (10 h, 1 d, 3 d, 6 d, and 10 d), the discs were collected from mice subcutaneously, washed with deionized water and dried in a vacuum oven at 35 °C for 3 d. Then the discs were dissolved in 20 mL of acetonitrile. Subsequently, 80 mL of methanol was added to precipitate the PCL polymer. By centrifuging the resulting suspension, a supernatant solution was obtained for drug concentration determination by HPLC. The drug releases percent was calculated according to the following formula:

$$\text{Drug relaese percent} = \left(1 - \frac{\text{Residual drug amout}}{\text{Intiial drug amount}}\right) \times 100\%$$

3. Results and discussion

3.1. Characterization of the drug-loaded films

3.1.1. Structures of the multilayered films

The bi-layered films were comprised of one drug layer and one backing layer. Two types of tri-layered films were prepared: (a) films with one backing layer, one drug layer and one drug-free PCL surface layer; and (b) films with one backing layer and two drug layers. The configurations of the bi-layered and tri-layered films are listed in Tables 2 and 3, respectively. The surfaces of the prepared films were flat and smooth before the release test (Fig. 1A), and the films presented obvious bi-layer or tri-layer architecture (Fig. 1B and C).

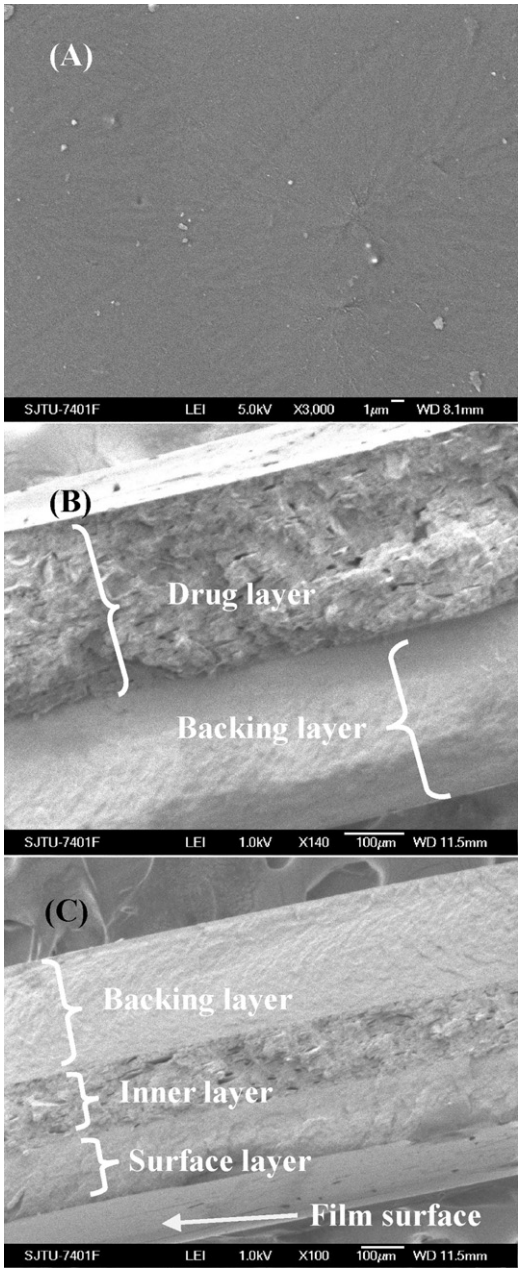

Fig. 1. SEM images of representative surface for the films before drug release (A) and cross-sections for bi/tri-layered films after 94 d drug release (B and C).

3.1.2. XRD patterns

As shown in Fig. 2A and B, PTX particles exhibited several intense peaks at 5.6°, 9.9° and 12.7°, which also corresponded to the data reported by Cavalcanti et al. (2007). 5-FU powders displayed high crystallinity as characterized by its sharp and intense diffraction peaks at 29° with a series of weak peaks between 21° and 32°, which were accordant with those reported by other literatures (Sairam et al., 2006). PCL film exhibited two characteristic peaks at 21° and 24°, confirming its semi-crystalline nature (Cheng et al., 2009). PEG displayed two distinct peaks at 19° and 23° (Cheng et al., 2010b). But the latter peak (at 23°) was hard to distinguish from one of the peaks for PCL at 24°. Therefore, the former peak (at 19°) was used to indicate the crystallinity of PEG in films. Films 6 and 7 had

Table 2
Configurations of the bi-layered films.

Film	Drug layer					Backing layer thickness (μm)
	PCL (w/w, %)	PEG (w/w, %)	5-FU (w/w, %)	PTX (w/w, %)	Thickness (μm)	
1	50	–	50	–	300	300
2	50	–	–	50	300	300
3	50	–	10	40	300	300
4	50	–	40	10	300	300
5	80	–	–	20	300	300
6	60	20	–	20	300	300
7	40	10	–	50	300	300

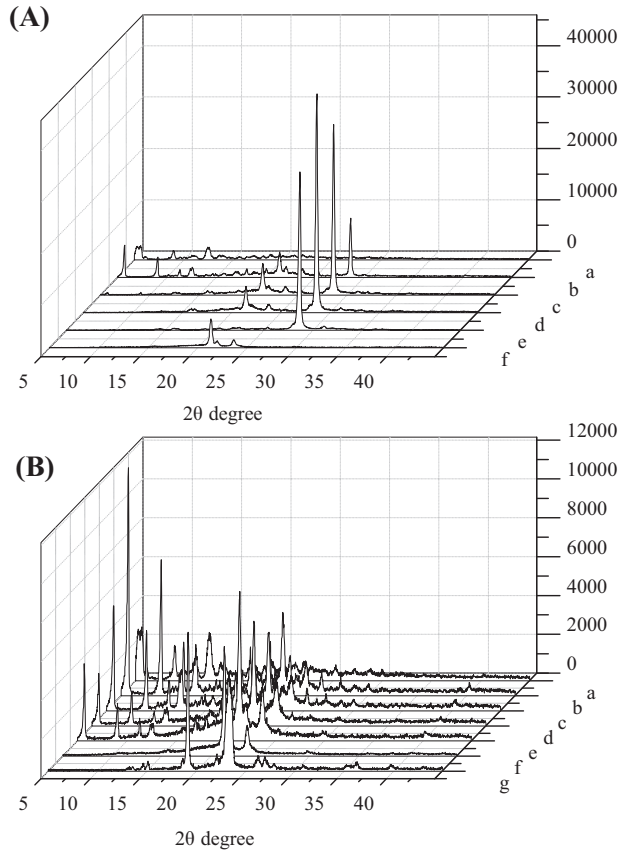

Fig. 2. XRD traces for PEG, PCL, 5-FU, PTX and all the single films. (A) PTX (a), Film III, IV and I (b–d) and 5-FU (e); (B) PTX (a), Film II, VII, VI and V (b–e), PCL (f), and PEG (g).

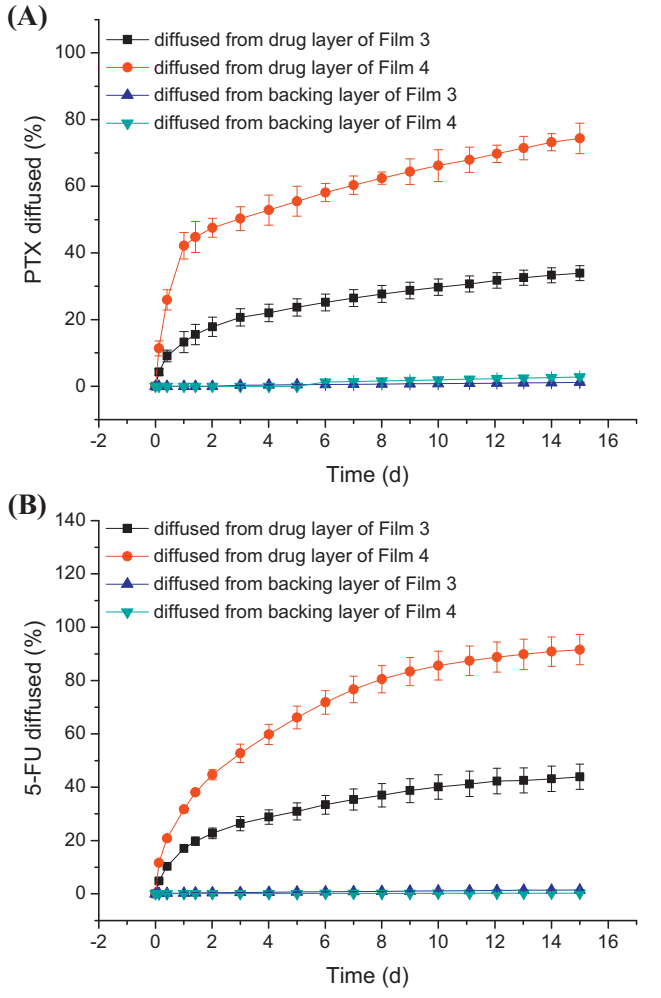

Fig. 3. Cumulative PTX and 5-FU diffusion curves for Films 3 and 4 (A and B). (Mean ± SD, $n = 3$.)

Table 3
Configurations of the tri-layered films.

Film	Surface layer					Inner layer					Backing layer thickness (μm)
	PCL (w/w %)	PEG (w/w, %)	5-FU (w/w, %)	PTX (w/w, %)	Thickness (μm)	PCL (w/w, %)	PEG (w/w, %)	5-FU (w/w, %)	PTX (w/w, %)	Thickness (μm)	
8	100	–	–	–	100	40	10	–	50	300	200
9	85	15	–	–	100	40	10	–	50	300	200
10	50	–	50	–	100	40	10	–	50	300	200
11	50	–	40	10	100	40	10	–	50	300	200
12	50	–	–	50	150	50	–	50	–	150	300
13	50	–	50	–	150	50	–	–	50	150	300

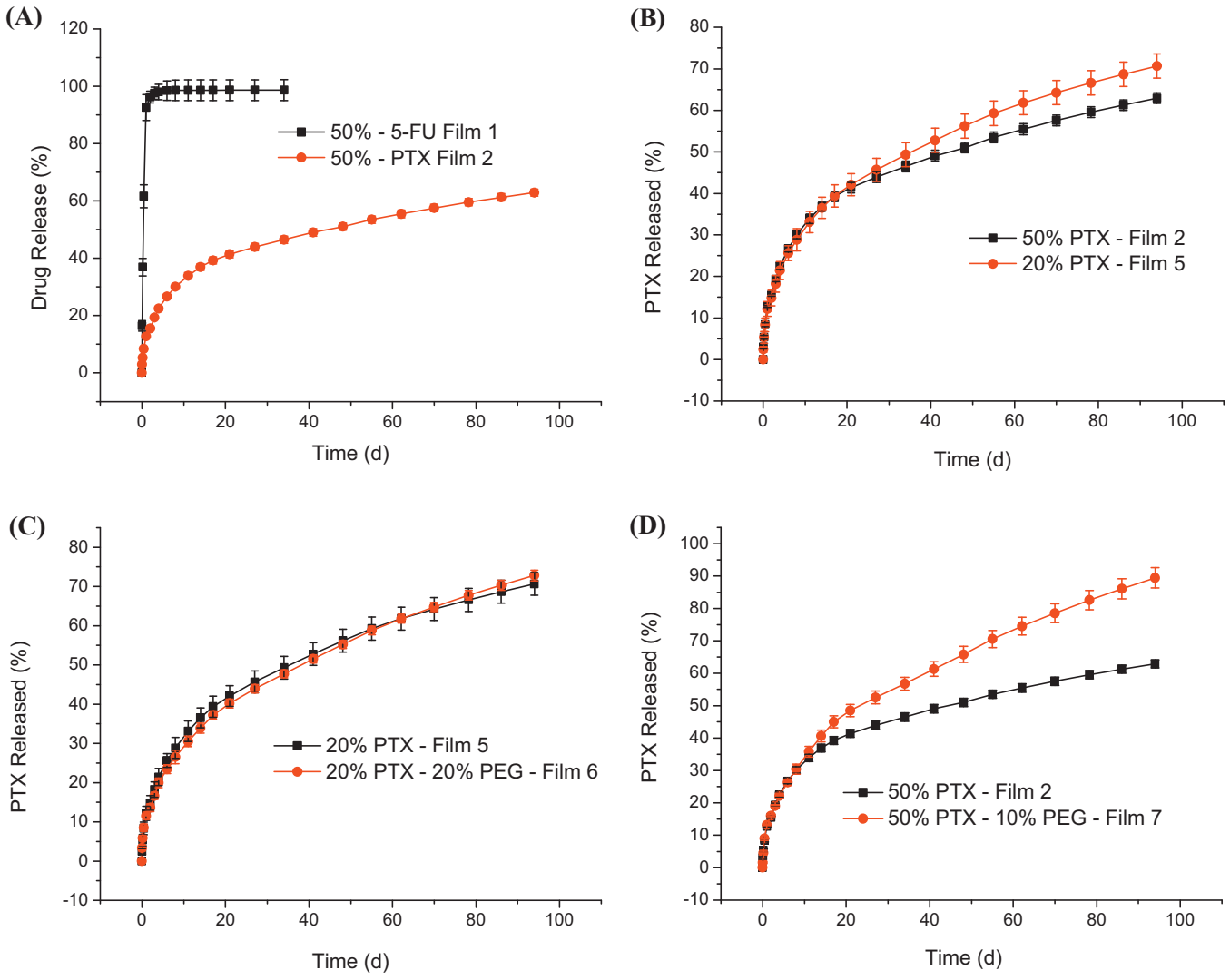

Fig. 4. Drug release profiles for the films: Films 1 and 2 (A), Films 2 and 5 (B), Films 5 and 6 (C), and Films 2 and 7 (D). (Mean ± SD, $n = 4$.)

weak diffractive peaks at 19°, showing PEG in PCL films was in its crystalline state. All PTX-loaded films showed characteristic peaks for PTX and all 5-FU-loaded films showed characteristic peaks for 5-FU as well, indicating that the incorporated drugs were in their crystalline states. It can be also observed that with the increase of drug loading, the intensities of the drug crystalline peaks in PCL films increased.

3.2. The role of backing layer in achieving unidirectional drug release

Horizontal diffusion cells test was carried out to examine the drug release and diffusion from the two sides (the drug layer and the backing layer) of the films. The drugs release/diffusion profiles are shown in Fig. 3A and B. It can be seen that 5-FU or PTX was released rapidly from the drug layer. However, the amounts of PTX or 5-FU diffused from the backing layer were almost zero during the investigated period, suggesting that the backing layer can effectively prevent drug release through it. Meanwhile, as shown in Fig. 1B and C, no pores or voids were generated in the backing layer after the 94-d drug release. As a contrast, it can be found that there exhibited many pores in the drug layer. These results suggested that the backing layer can endow the film with unidirectional drug release property.

3.3. Effect of film formulations on drug release

3.3.1. Hydrophilic 5-FU and hydrophobic PTX

5-FU is a hydrophilic drug, and PTX is a hydrophobic drug. They may have different release behaviors from PCL matrix. Here we investigated the PCL films loaded with 50% of 5-FU or 50% of PTX. As presented in Fig. 4A, 5-FU was released much faster than PTX from PCL matrix, suggesting that hydrophilic 5-FU could diffuse faster than hydrophobic PTX. It indicated that drug release behaviors from the PCL matrix were partly related to their physical and chemical properties.

3.3.2. Effect of drug loading on drug release

In order to investigate the influence of drug loading on drug release in our multi-layered films, similarity factor (f_2) (Costa et al., 2001), as determined by FDA and EMEA, was introduced to compare the release profiles:

$$f_2 = 50 \times \log\left\{\left[1 + \frac{1}{n}\sum_{t=1}^{n} W_t |R_t - T_t|^2\right]^{-0.5} \times 100\right\}$$

where w_t is an optional weight factor and was taken as 1 in our study, since all the investigated release time points are treated

equally. The similarity factor is 100 when the test and reference profiles are identical and tends to 0 as the dissimilarity increases. FDA and EMEA suggest that two dissolution profiles are declared similar if f_2 is between 50 and 100.

PCL films with two PTX contents (20% and 50%) (Films 2 and 5) were investigated. Fig. 4B shows that there was no apparent difference between PTX release profiles for the two films (f_2 = 70.3), suggesting that drug loading had no significant influence on PTX release from the two films. In our previous work (Lei et al., 2010), we have investigated the effect of drug loading on drug release for the PCL film loaded with 5-FU, and there was no obvious difference on 5-FU release from the two films loaded with 20% and 40% of 5-FU, but when drug content increased to 60%, 5-FU release became much faster. These phenomena have been reported and explained using drug percolation threshold (Guo et al., 2007; Petrovic et al., 2009).

3.3.3. Effect of PEG addition on the drug release

It can be observed from Fig. 4C and D that the effect of PEG addition on PTX release was related to drug loading. For Films 5 and 6 with 20% PTX (Film 5 contained no PEG and Film 6 contained 20% PEG), their PTX release profiles were almost the same (f_2 = 86.7), indicating no effect of PEG addition on PTX release. However, for Films 2 and 7 with 50% PTX (Film 2 contained no PEG and Film 7 contained 10% PEG), PTX was released faster from Film 7 than that from Film 2 (f_2 = 45.5), suggesting that the addition of PEG accelerated PTX release. This may be explained by the added PEG interconnects the discrete PTX particles in PCL films with a relative high drug loading (50%), and PEG was released rapidly when the films was placed in PBS medium, leaving microcavities or channels connecting PTX particles. Subsequently, water diffused quickly into the films through these microcavities or channels, which in turn allowed rapid dissolution and diffusion of PTX particles. As a comparison, it was reported that 5-FU (with a relative high drug loading of 40%) release could be accelerated tremendously due to the added PEG as well as be regulated by the amount of PEG in PCL film (Lei et al., 2010). These results suggested that the added PEG could promote drug release from PCL films with relative high drug loadings.

3.3.4. Effect of 5-FU/PTX ratio on drug release

The drug release behaviors of Films 3 and 4, whose drug-loaded layers contained both 5-FU and PTX, were analyzed. The total drug loadings of the two films were 50%. Film 3 contained 40% PTX and 10% 5-FU, while Film 4 contained 10% PTX and 40% 5-FU. PTX and 5-FU release profiles are presented in Fig. 5A and B, respectively. PTX was released much faster from Film 4 than that from Film 3. PTX release from Film 2 containing 50% PTX was similar to that from Film 3 but much slower than that from Film 4. 5-FU release from Film 4 was also faster than that from Film 3 but a little slower than that from Film 1 containing 50% 5-FU. These results implied that the release of PTX from the PCL films with a high ratio of 5-FU/PTX was fast, and the release of 5-FU from the PCL films with a low ratio of 5-FU/PTX was slowed down. As hydrophilic 5-FU was released much faster than PTX from the PCL matrix, the effect of 5-FU release on PTX release would be greater than that of PTX release on 5-FU release from the PCL films. This is because a greater number of pores were left after 5-FU release (Fig. 7F), which made PTX be released faster from PCL matrix. These release profiles demonstrated that the release of 5-FU and PTX could be adjusted by altering the ratio of 5-FU/PTX.

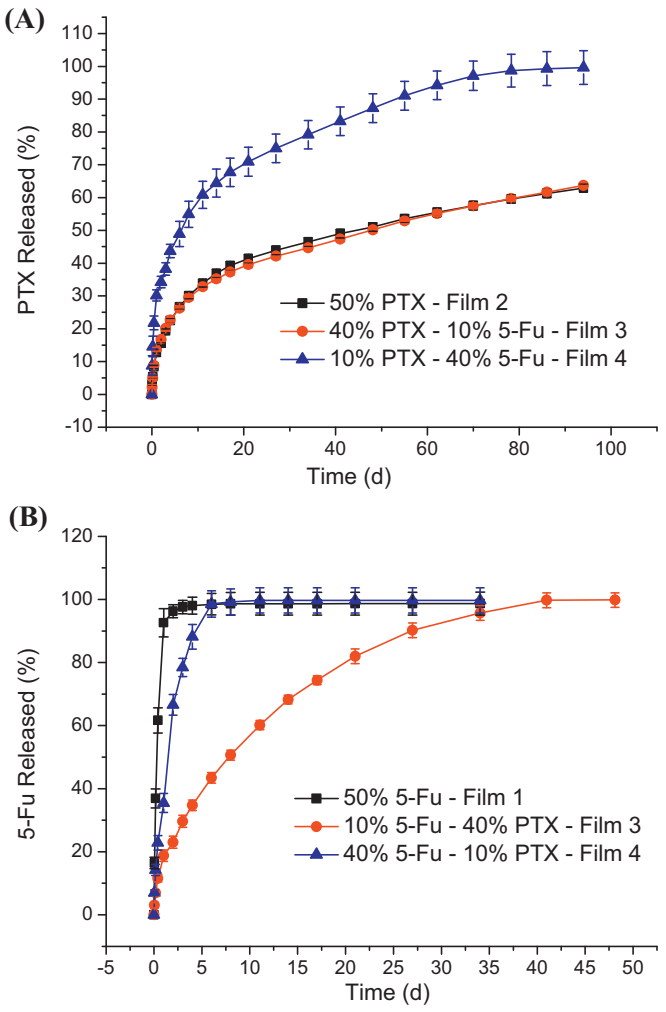

Fig. 5. PTX release profiles for Films 2–4 (A); 5-FU release profiles of Films 1, 3 and 4 (B). (Mean ± SD, n = 4.)

3.4. Effect of film architecture on drug release

3.4.1. Effect of surface layer on PTX release

The tri-layered films (Films 8–11) were obtained by agglutinating one surface layer (100 μm thick PCL based film) with the drug layer of the bi-layered film (Film 7). Their configurations are listed in Table 3. As shown in Fig. 6A, PTX release profiles for the tri-layered films (Films 8–11) were different from that for the bi-layered film (Film 7). PTX was released slower from the tri-layered films than that from the bi-layered film. The slowing down of PTX release was associated with the composition of the surface layer. Films 8 and 9 with drug-free surface layers had similar PTX release profiles. Both of them released PTX slower than Film 10 or 11. It indicated that the drug-free surface layers can greatly slow down drug release from the inner layers. Compared with PTX, 5-FU was released much faster from the surface layer (almost released completely in 24 h), as shown in Fig. 6B. Many pores or voids were generated in surface layer after 5-FU release, which would be beneficial to the diffusion of PTX in the inner layer through the surface layer. This might be the reason that PTX was released a little faster from Film 10 or 11 than that from Films 8 and 9. PTX was released slightly faster from Film 11 than that from Film 10, because the surface layer of Film 11 also contained 10% PTX. It indicated that drug release can be effectively tuned by agglutinating surface layer with different compositions onto the bi-layered films.

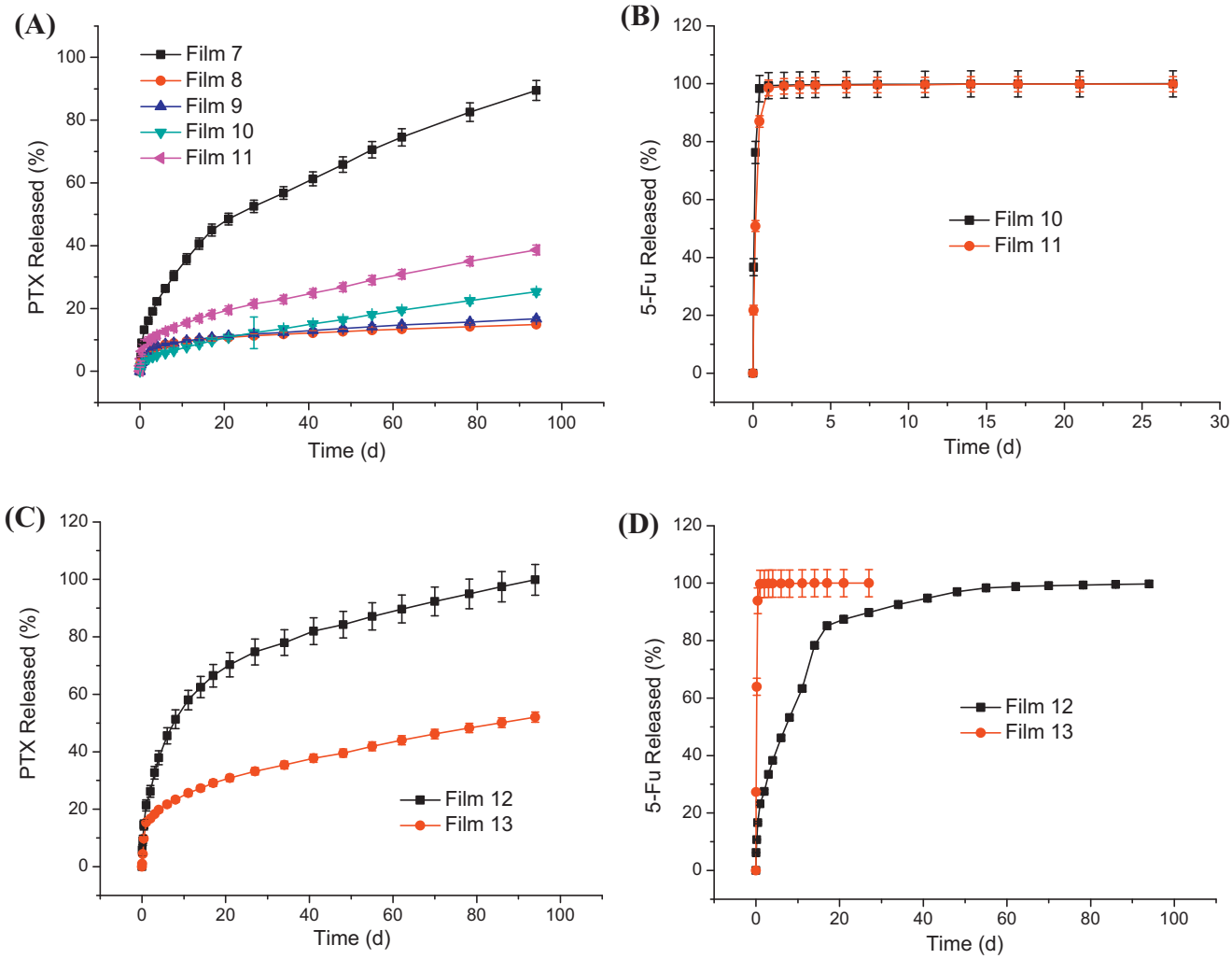

Fig. 6. PTX release profiles for Films 7–11 (A); 5-FU release profiles for Films 10 and 11 (B); PTX release profiles for Film 2, 12 and 13 (C); 5-FU release profiles for Films 1, 12 and 13 (D). (Mean ± SD, $n = 4$.)

PTX release kinetics was analyzed by the Higuchi model (Higuchi, 1961) and the Ritger–Peppas model (Ritger and Peppas, 1987). The n value of the Ritger–Peppas model is the diffusional exponent indicative of the release mechanism. In the case of film dosage form, the n value is 0.5 for Fickian diffusion, while 1 for Case-II transport; when the n value is between 0.5 and 1, the drug release mechanism is anomalous (non-Fickian) transport (Lei et al., 2010). As shown in Table 4, the obtained n values for Films 8, 9 and 11 were all less than 0.5 and the n value for Film 10 was close to 0.5, indicating that Fickian diffusion is the predominant release mechanism for the films.

3.4.2. *Effect of 5-FU/PTX incorporated in surface/inner layer on drug release*

There were two drug layers and one backing layer for Films 12 and 13 which had the same PTX or 5-FU contents. The drug loading modes of the two films were different. For Film 12, the surface layer contained 50% PTX and the inner layer contained 50% 5-FU; for Film 13, the surface layer contained 50% 5-FU and the inner layer contained 50% PTX. As illustrated in Fig. 6C and D, PTX was released faster from Film 12 than that from Film 13, and 5-FU was released slower from Film 12 than that from Film 13. These results indicated that drug incorporated in surface layer was easier to be released

Table 4
Fitting results of the PTX release data by Ritger–Peppas and Higuchi models.

Film	Time period (days)	Ritger–Peppas model ($(M_t/M_\infty) = kt^n$)[a]			Higuchi model ($(M_t/M_\infty) = kt^{0.5}$)[a]	
		n	k	r	k	r
Film 8	0–94	0.242	0.050	0.993	0.019	0.811
Film 9	0–94	0.270	0.049	0.994	0.021	0.876
Film 10	0–94	0.529	0.022	0.997	0.025	0.997
Film 11	0–94	0.387	0.063	0.994	0.041	0.980

[a] M_t/M_∞, fractional drug release; t, the release time; k, a constant of the drug–polymer system; n, diffusional exponent; r, correlation coefficient.

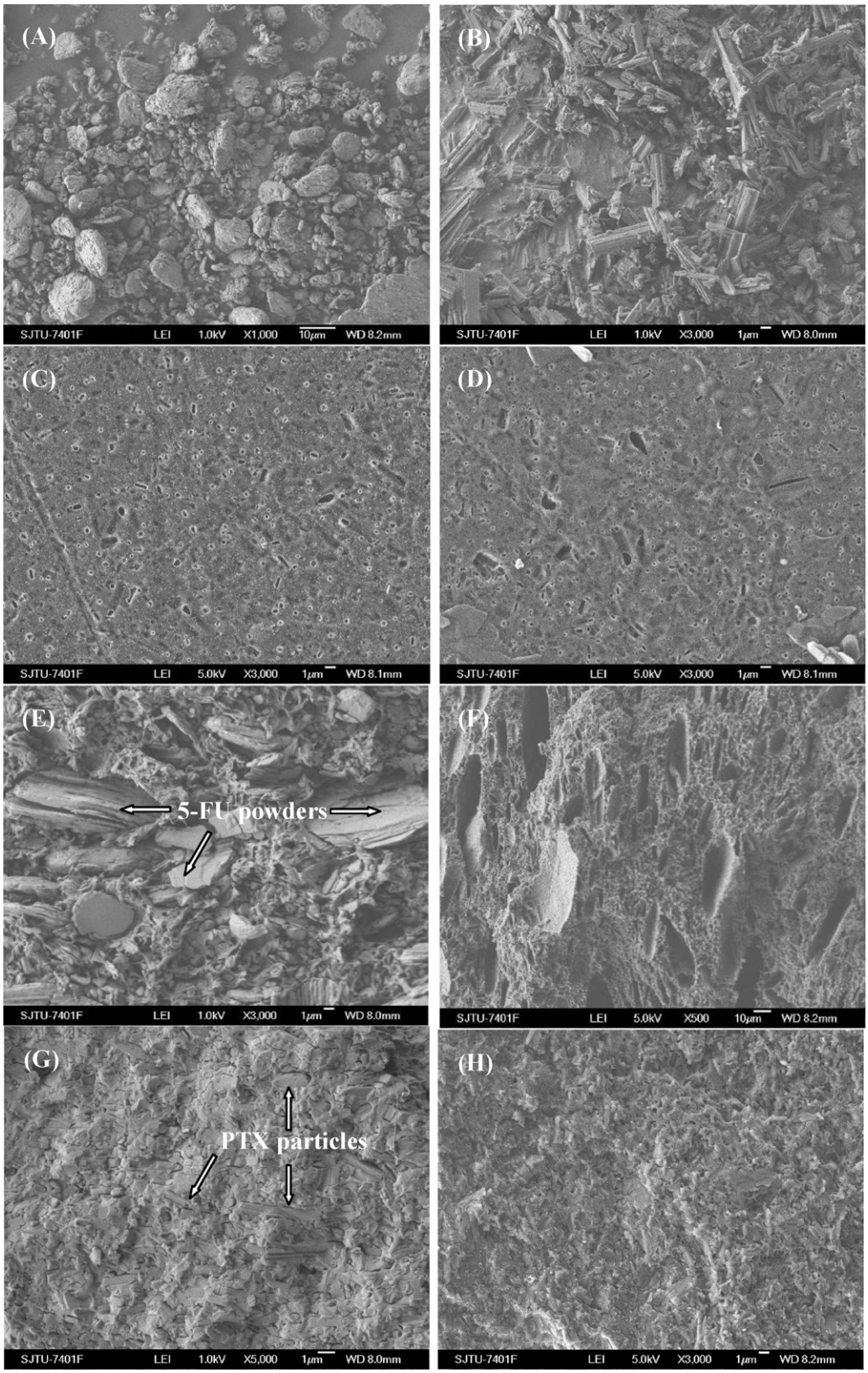

Fig. 7. SEM images of 5-FU and PTX particles (A and B); surface for Films 2 and 3 after 94 d drug release (C and D); cross-section morphologies for the films before and after drug release (E and F for Film 1; G and H for Film 2).

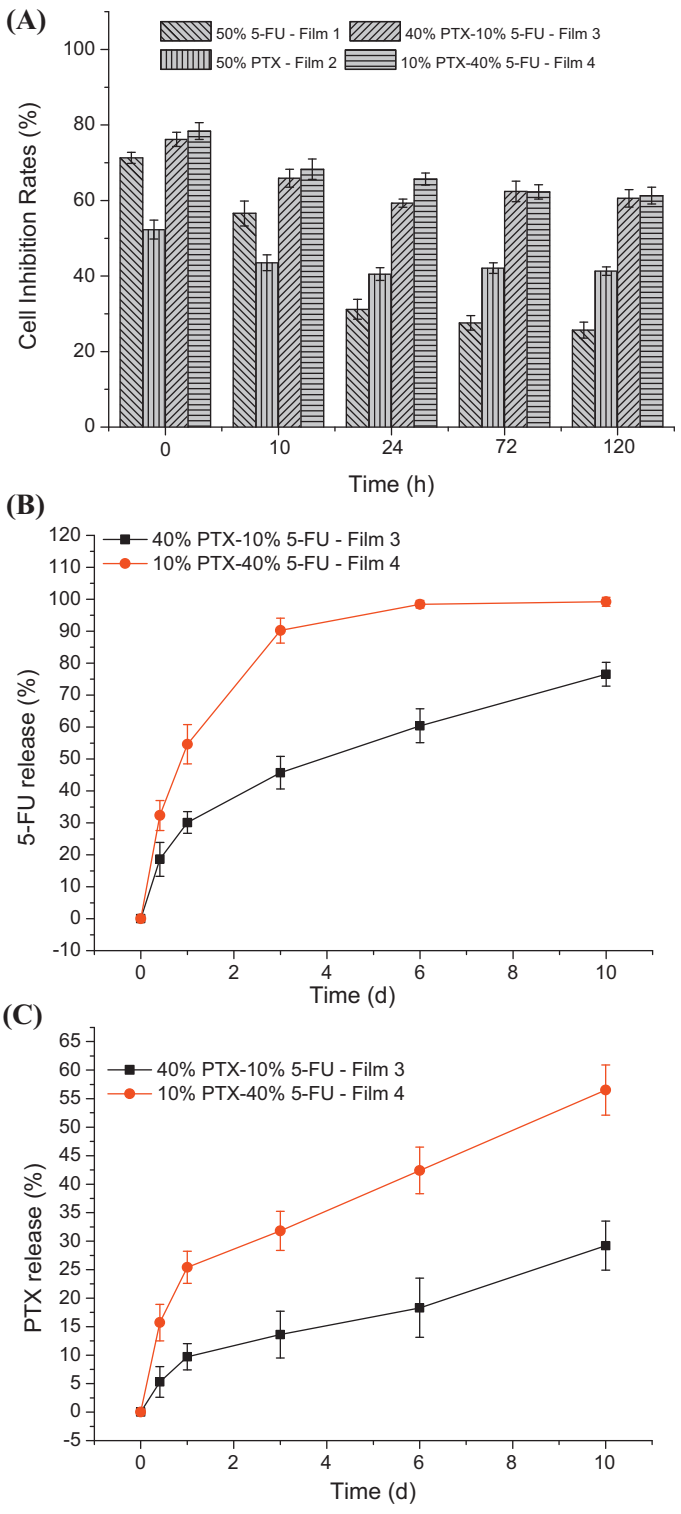

Fig. 8. MTT assay results (A); *in vivo* 5-FU releases for Films 3 and 4 (B); *in vivo* PTX releases for Films 3 and 4 (C).

than that in inner layer, and the fast release of 5-FU could be alleviated by the addition of surface layer loaded with the hydrophobic PTX.

3.5. Film surface and bulk morphologies

The surface and bulk morphologies of films, investigated by SEM, are shown in Fig. 7. 5-FU particles were irregular and PTX particles were prismatic, which were both smaller than 10 μm (Fig. 7A and B). Generally, the surfaces for all the prepared films were compact and smooth before drug release (Fig. 1A). After drug release, however, the surfaces presented various numbers of tiny pores and became rough (Fig. 7C and D). These pores might be generated by the leakage of drug particles located near the surface and the erosion of the PCL matrix.

As shown in Fig. 7E or G, 5-FU or PTX particles could be observed on the film cross-section and their crystals were homogeneously distributed in PCL matrix. These were in accordance with the XRD results showing the existence of 5-FU and PTX crystals. After drug release, many discrete pores could be observed in the drug-loaded layer (Fig. 7F or H), and the size and shape of these pores were nearly identical to that of 5-FU or PTX particles, respectively, suggesting that these pores were left by the released drug. As discussed above, 5-FU was released much faster than PTX from the PCL film. Thus, the pores which were generated by the release of 5-FU particles, could promote PTX release in the later stage. This may account for the drug release result that PTX was released faster from Film 10 than that from Film 8 or 9 in the later stage (Fig. 6A).

3.6. Cell toxicity

As seen in Fig. 8A, the viability of Eca-109 cells was inhibited by 25–78%, depending on the film composition and drug release times, showing that the films can effectively inhibit the proliferation of Eca-109 cells. It can be also found that the films could sustain their cytotoxicity for a prolonged time. The cell inhibition rates for Film 1 containing 50% 5-FU decreased as the release time increased. This is because that less drug was left in the films after a longer drug release time. However, the cell inhibition rates for Film 2 containing 50% PTX did not obviously decrease as the drug release time extended from 10 to 120 h. This might be due to slow release of PTX from the film. In the investigated period (120 h), the amount of 5-FU released was much larger than that of PTX released (shown in Fig. 4A). Thus, the drug release rate has a significant effect on the cell inhibition ability for Film 1 and no obvious effect for Film 2. Films 3 and 4 containing both 5-FU and PTX have high cell inhibition rates even after drug release for 120 h.

3.7. In vivo release

As shown in Fig. 8B and C, the *in vivo* releases for 5-FU and PTX from Film 4 were faster than those from Film 3, which were corresponded with the *in vitro* 5-FU and PTX release profiles for Films 3 and 4 (shown in Fig. 5). 76.5% and 99.2% of the incorporated 5-FU were released from Films 3 and 4 after 10 d, respectively. However, only 29.2% and 56.5% of PTX were released from Films 3 and 4 after 10 d, respectively. Thus, 5-FU was released from the film faster than PTX. These *in vivo* results are correlative with the *in vitro* drug release profiles for the PCL films.

4. Conclusion

The bi/tri-layered films co-loaded with 5-FU and PTX were successfully prepared. 5-FU was released much faster than PTX from the films. The backing layer can endow the films with unidirectional drugs release characteristic. For multi-layered films co-loaded with both 5-FU and PTX, pores generated by the release of 5-FU particles could promote the release of PTX in the later stage. The introduction of surface layer can effectively adjust the drug release from the inner layer of the tri-layered film. Besides, the drug release could be further regulated by changing the drug loading, and by the addition of PEG. The application of multiple drug layers with different drug formulations and spacial architectures could effectively enrich the variability of drug release. The *in vivo* and *in vitro* drug releases for

the PCL films incorporated with PTX/5-FU are highly correlative. Owing to the characteristic of unidirectional and rate-tunable drug release and dual drug loading capacity, the multi-layered PCL films co-loaded with 5-FU and PTX can be an attractive drug delivery system for intraluminal tumor treatment.

Acknowledgements

This work was supported by Shanghai Science and Technology Committee (10441902000), the National Key Program for Basic Research of China (2010CB529902) and the Key Program of the Shanghai Municipal Education Committee (09ZZ24). The authors would like to thank Instrumental Analysis Center of Shanghai Jiao Tong University for their technical support.

References

Ako, J., Bonneau, H.N., Honda, Y., Fitzgerald, P.J., 2007. Design criteria for the ideal drug-eluting stent. Am. J. Cardiol. 100, 3M–9M.

Cavalcanti, L.P., Konovalov, O., Haas, H., 2007. X-ray diffraction from paclitaxel-loaded zwitterionic and cationic model membranes. Chem. Phys. Lipids 150, 58–65.

Chen, W.L., Shen, Y.Y., Rong, H.J., Lei, L., Guo, S.R., 2012. Development and application of a validated gradient elution HPLC method for simultaneous determination of 5-fluorouracil and paclitaxel in dissolution samples of 5-fluorouracil/paclitaxel-co-eluting stents. J. Pharm. Biomed. Anal. 59, 179–183.

Cheng, L., Guo, S.R., Wu, W.P., 2009. Characterization and in vitro release of praziquantel from poly(epsilon-caprolactone) implants. Int. J. Pharm. 377, 112–119.

Cheng, L., Lei, L., Guo, S., 2010a. In vitro and in vivo evaluation of praziquantel loaded implants based on PEG/PCL blends. Int. J. Pharm. 387, 129–138.

Cheng, L., Lei, L., Guo, S.R., 2010b. In vitro and in vivo evaluation of praziquantel loaded implants based on PEG/PCL blends. Int. J. Pharm. 387, 129–138.

Costa, P., Manuel, J., Lobo, S., 2001. Modeling and comparison of dissolution profiles. Eur. J. Pharm. Sci. 13, 123–133.

Feng, J.-F., Lu, J.-W., Sun, X.-F., 2004. Biweekly regimen of high dose of leucovorin, 5-fluorouracil, and paclitaxel for patients with advanced gastric cancer. Ai Zheng 23, 1704–1706.

Guo, Q.H., Guo, S.R., Wang, Z.M., 2007. Estimation of 5-fluorouracil-loaded ethylene-vinyl acetate stent coating based on percolation thresholds. Int. J. Pharm. 333, 95–102.

Guo, Q.Y., Knight, P.T., Mather, P.T., 2009. Tailored drug release from biodegradable stent coatings based on hybrid polyurethanes. J. Control. Release 137, 224–233.

Gupta, R.S., 1985. Cross-resistance of vinblastine- and taxol-resistant mutants of Chinese hamster ovary cells to other anticancer drugs. Cancer Treat. Rep. 69, 515–521.

Gupte, A., Ciftci, K., 2004. Formulation and characterization of paclitaxel, 5-FU and paclitaxel+5-FU microspheres. Int. J. Pharm. 276, 93–106.

Higuchi, T., 1961. Rate of release of medicaments from ointment bases containing drugs in suspension. J. Pharm. Sci. 50, 874–875.

Lee, J.-W., Park, J.-K., Lee, S.-H., Kim, S.-Y., Cho, Y.-B., Kuh, H.-J., 2006. Anti-tumor activity of heptaplatin in combination with 5-fluorouracil or paclitaxel against human head and neck cancer cells in vitro. Anticancer Drugs 17, 377–384.

Lei, L., Guo, S.R., Chen, W.L., Rong, H.J., Lu, F., 2011a. Stents as a platform for drug delivery. Expert. Opin. Drug Deliv. 8, 813–831.

Lei, L., Liu, X., Guo, S.R., Tang, M.F., Cheng, L.A., Tian, L., 2010. 5-Fluorouracil-loaded multilayered films for drug controlled releasing stent application: drug release, microstructure, and ex vivo permeation behaviors. J. Control. Release 146, 45–53.

Lei, L., Liu, X., Shen, Y.Y., Liu, J.Y., Tang, M.F., Wang, Z.M., Guo, S.R., Cheng, L., 2011b. Zero-order release of 5-fluorouracil from PCL-based films featuring trilayered structures for stent application. Eur. J. Pharm. Biopharm. 78, 49–57.

Little, U., Buchanan, F., Harkin-Jones, E., McCaigue, M., Farrar, D., Dickson, G., 2009. Accelerated degradation behaviour of poly(epsilon-caprolactone) via melt blending with poly(aspartic acid-co-lactide) (PAL). Polym. Degrad. Stab. 94, 213–220.

Liu, X., Lei, L., Hou, J.W., Tang, M.F., Guo, S.R., Wang, Z.M., Chen, K.M., 2011. Evaluation of two polymeric blends (EVA/PLA and EVA/PEG) as coating film materials for paclitaxel-eluting stent application. J. Mater. Sci. Mater. Med. 22, 327–337.

Longley, D.B., Harkin, D.P., Johnston, P.G., 2003. 5-Fluorouracil: mechanisms of action and clinical strategies. Nat. Rev. Cancer 3, 330–338.

Monsuez, J.J., Charniot, J.C., Vignat, N., Artigou, J.Y., 2010. Cardiac side-effects of cancer chemotherapy. Int. J. Cardiol. 144, 3–15.

Petrovic, J., Ibric, S., Jockovic, J., Parojcic, J., Duric, Z., 2009. Determination of the percolation thresholds for polyethylene oxide and polyacrylic acid matrix tablets. J. Drug Deliv. Sci. Technol. 19, 359–364.

Ritger, P.L., Peppas, N.A., 1987. A simple equation for description of solute release II. Fickian and anomalous release from swellable devices. J. Control. Release 5, 37–42.

Rohner, D., Hutmacher, D.W., See, P., Tan, K.C., Yeow, V., Tan, S.Y., Lee, S.T., Hammer, B., 2002. Individually CAD-CAM technique designed, bioresorbable 3-dimensional polycaprolactone framework for experimental reconstruction of craniofacial defects in the pig. Mund Kiefer Gesichtschir. 6, 162–167.

Sairam, M., Babu, V.R., Naidu, B.V.K., Aminabhavi, T.M., 2006. Encapsulation efficiency and controlled release characteristics of crosslinked polyacrylamide particles. Int. J. Pharm. 320, 131–136.

Sinha, V.R., Bansal, K., Kaushik, R., Kumria, R., Trehan, A., 2004. Poly-epsilon-caprolactone microspheres and nanospheres: an overview. Int. J. Pharm. 278, 1–23.

Sugimura, M., Sagae, S., Ishioka, S., Nishioka, Y., Tsukada, K., Kudo, R., 2004. Mechanisms of paclitaxel-induced apoptosis in an ovarian cancer cell line and its paclitaxel-resistant clone. Oncology 66, 53–61.

Tsuji, T., Tamai, H., Igaki, K., Kyo, E., Kosuga, K., Hata, T., Nakamura, T., Fujita, S., Takeda, S., Motohara, S., Uehata, H., 2003. Biodegradable stents as a platform to drug loading. Int. J. Cardiovasc. Intervent. 5, 13–16.

Waksman, R., Wakabayashi, K., 2010. Biodegradable polymer for drug-eluting stents—a true advantage or only perception? Circ. J. 74, 2052–2053.

Watari, H., Hosaka, M., Mitamura, T., Moriwaki, M., Ohba, Y., Todo, Y., Takeda, M., Ebina, Y., Sakuragi, N., 2008. Weekly paclitaxel/5-fluorouracil followed by platinum retreatment for patients with recurrent ovarian cancer: a single institution experience. Eur. J. Gynaecol. Oncol. 29, 573–577.

Zilberman, M., Eberhart, R.C., 2006. Drug-eluting bioresorbable stents for various applications. Annu. Rev. Biomed. Eng., 153–180.